Wavelet-based no-reference blocking artifact measure

Seungchul Ryu and *Kwanghoon Sohn

Digital Image Media Laboratory (DIML)
School of Electrical and Electronic Engineering, Yonsei Univerity
Seoul, Republic of Korea
ryus01@yonsei.ac.kr and *khsohn@yonsei.ac.kr

***Abstract*—A blocking artifact is the most common artifact in the image and video compression, such as JPEG, MPEG-2, and H.264. This paper presents an objective metric for measuring a blocking artifact in an image. The proposed method does not require a reference image and thus is applicable to many practical applications in which no reference image is available. In the proposed metric, an objective blockiness score is computed based on the properties of local wavelet coefficients. Simulation results and comparisons with existing no-reference blockiness metrics proved that the proposed metric correlates well with the perceived subjective scores and outperforms the existing metrics.**

Index terms; wavelet, no-reference, blocking artifact

I. INTRODUCTION

The quantization of DCT coefficients is an effective technique to reduce bitrates that have to be transmitted in block-based video coding standards, such as JPEG, MPEG-2, and H.264. However, a coarse quantization may result in the blocking artifacts within the decoded image and video. Subjective experiments have indicated that the blocking artifact is the most annoying distortion at low and moderate bitrates in JPEG and MPEG-2 [1-2]. Accordingly, the measurement of the blocking artifact is important task in the design and optimization of the coding system, and a quality assessment of image and video.

The subjective method is considered as the most reliable approach in a quality assessment of an image because the end user is generally human being in many practical applications. However, the subjective method is impractical for real-time application since it requires unreasonable cost and time. Therefore, many objective metrics have been proposed in the last decades. Objective metrics can be divided into three categories according to the amount of referred information about the original image: full-reference, reduced-reference, and no-reference methods [3]. Among these quality assessment methods, no-reference methods are highly desired in environments where the reference image is not available.

In the last decades, several no-reference metrics for measuring blocking artifacts have been proposed in literature [4-11]. Wu and Yuen [4] proposed a Generalized Block Impairment Metric (GBIM) that exploiting perceptual features, such as texture and luminance masking. The metric models the blockiness as the inter-pixel difference across block boundaries with simple texture and luminance masking models. In [5], blockiness metric is proposed based on the 1-D pixel vectors across two adjacent blocks. The blockiness is computed using the relative ratio of slopes between boundary and internal pixels in the 1-D pixel vector. In [6], Wang and Bovik modeled the blocky image as a non-block image interfered with a pure blocky distortion. Then, the strength of block-edges is computed based on the FFT along the rows and columns considering the luminance and texture masking.

In [7], the authors proposed the blockiness metric based on a locally adaptive algorithm. In the method, the blockiness and the flatness is combined into a perceptual blockiness score with the local contrast masking and spatial masking. In [8], the authors proposed simple cost-effective grid detection and blocking artifact measure. They are used to suppress blocking artifact while preserving the sharpness of object edges. In [9], a noticeable blockiness map is constructed from the block discontinuity map considering the effects of the luminance adaptation and texture masking. Then, the overall perceptual blockiness is computed using a nonlinear operator. Recently, a novel approach [10-11] is proposed including grid detection algorithm and visual masking model. The blockiness is calculated by local pixel-based blocking artifact model combined with its local visibility and grid detector.

In this paper, we propose a new approach for measuring the blocking artifact in images and videos. The proposed metric exploits the properties varied according to the degree of blocking artifacts present within an image.

(a) (b) (c) (d) (e)

Fig. 1 Enlarged JPEG-coded 'womanhat' images at (a) 1.47 bits/pixel, (b) 0.60 bits/pixel, (c) 0.45 bits/pixel, (d) 0.33 bits/pixel, and (e) 0.16 bits/pixel.

This paper is organized as follows. Section II describes the proposed no-reference blocking artifact metric. The efficiency of the proposed metric is evaluated for public LIVE image database [12] in Section III. A conclusion of this paper is followed in Section IV.

II. Proposed Method for Mesuring Blocking Artifact

At low bitrates, the DCT-based lossy compression methods cause severe blocking artifacts due to a coarse quantization for most DCT coefficients close to zeros. Fig. 1 shows examples of blocking artifacts. They are the enlarged JPEG-coded 'womanhat' images at 1.47 bits/pixel, 0.60 bits/pixel, 0.45 bits/pixel, 0.33 bits/pixel, and 0.16 bits/pixel, respectively. As shown in Fig. 1, the blocking artifacts seriously degrade the visual quality especially at low bitrates.

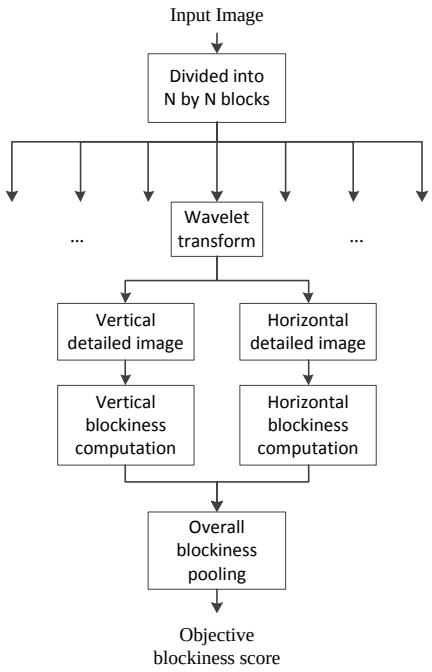

Fig. 2 Overall flow-diagram of the proposed metric

Fig. 2 illustrates the overall process of the proposed metric. First, an image is divided into N × N square blocks. Each block is then transformed into wavelet domain which consists of approximated, horizontal detailed, vertical detailed and diagonal detailed images. The local horizontal and vertical blockiness are computed by the horizontal and vertical detailed images, respectively. Then, they are used to provide an overall blockiness score.

The properties of wavelet images are varied according to the degree of a blocking artifact. A few examples are shown in Fig. 3 and Fig. 4. 'womanhat' images in spatial domain without and with severe blocking artifact are shown in Fig.3 (a) and Fig. 4 (a), respectively. The wavelet transformed images are presented in Fig. 3 (b)-(e) and Fig. 4 (b)-(e), respectively. Accumulated histograms of detailed images are also shown at the rightmost in Fig. 3 and Fig. 4.

Fig.3 (f) and Fig. 4 (f) show accumulated histograms of horizontal detailed image into vertical direction while Fig. 3 (g) and Fig. 4 (g) show accumulated histograms of vertical detailed image into horizontal direction. The figures show that the blocking artifact makes the histogram sparser with high-amplitude of peaks and low-amplitude of non-peaks. The accumulated histograms are computed as follows;

$$h_h(i) = \sum_{j}^{N} \left| w_h(i,j) \right|, \tag{1}$$

$$h_v(i) = \sum_{i}^{N} \left| w_v(i,j) \right|, \tag{2}$$

where $h_h(i)$ is the accumulated histogram of horizontal detailed image into vertical direction, $h_v(i)$ is the accumulated histogram of vertical detailed image into horizontal direction. In addition, N, $w_h(i,j)$, and $w_v(i,j)$ are

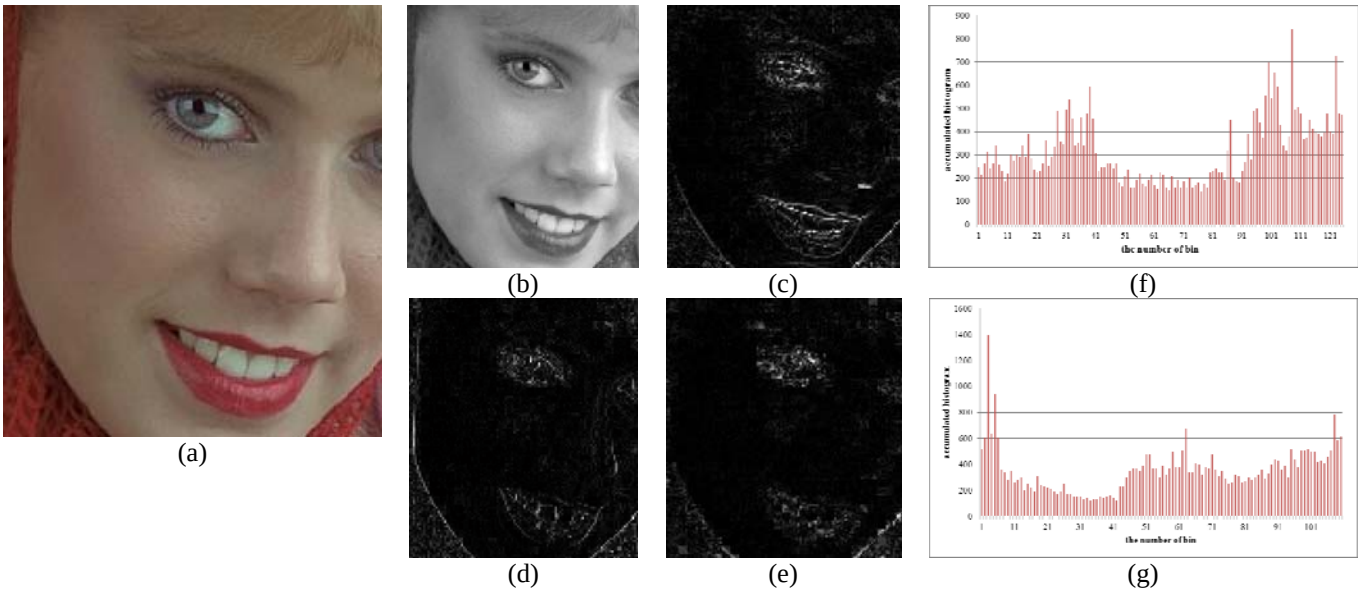

Fig. 3 (a) original 'womanhat' image, (b)-(e) wavelet transformed images: (b) approximated image; (c) horizontal detailed image; (d) vertical detailed image; (e) diagonal detailed image, (f) accumulated histogram of horizontal image into vertical direction, (g) accumulated histogram of vertical image into horizontal direction.

the size of a local block, the horizontal detailed image, the vertical detailed image, respectively.

The accumulated histograms are used to derive local blockiness scores as follows;

$$lb_h = \frac{\frac{1}{M_1}\sum_{k}^{M_1} np_h(k)}{\frac{1}{M_2}\sum_{k}^{M_2} p_h(k) + C_1}, \quad (3)$$

$$lb_v = \frac{\frac{1}{M_1}\sum_{k}^{M_1} np_v(k)}{\frac{1}{M_2}\sum_{k}^{M_2} p_v(k) + C_1}, \quad (4)$$

where lb_h and lb_v are a local horizontal and vertical blockiness scores. *np(k)* and *p(k)* are non-peak bins and peak bins. M_1 and M_2 are the number of non-peak bins and the number of peak bins, respectively. The peak and non-peak bins are determined by a simple thresholding method. Note that C_1 (C_1=0.1) is just used for stability of the equations.

The local blockiness scores are summed up to produce an overall blockiness index *B* as follows;

$$B = \alpha\left(\frac{1}{N_b}\sum_{l}^{N_b} lb_h(l)\right) + (1-\alpha)\left(\frac{1}{N_b}\sum_{l}^{N_b} lb_v(l)\right), \quad (5)$$

where N_b is the number of local blocks. Here, we assume that the influences of the horizontal and vertical blockiness for the overall quality are same. Thus, α=0.5 is used in (5).

III. Performance Evaluation

To validate the performance of the proposed blockiness metric, the LIVE JPEG database [12] which consists of 233 JPEG images with their Difference Mean Opinion Score (DMOS) is used. The evaluations are conducted comparing four existing no-reference blockiness metrics including the most referred three metrics [4, 6, 7] and the most recent metric [11]. Note that we refer [4] as GIBM, [6] as BBAM, [7] as LABM, and [11] as PBM for convenience.

The testing beds consist of two scenarios as follows; 1) Test 1: In this test, the capability of prediction for images including same contents with different degree of blocking artifacts is evaluated. It consists of five JPEG-compressed 'womanhat' images shown in Fig. 1 and uncompressed original image, totally six images. 2) Test 2: In this test, we evaluate the performances of the metrics when they are applied to images having different contents using 233 LIVE JPEG-compressed images.

Fig. 5 shows the results of the metrics when applied to 'womanhat' images (Test 1). As expected, all the metrics are monotonically increase or decrease as blocking artifacts increase even though the prediction accuracies are varied. Note that all the metrics increase as the blocking artifact is incremented except for PBM [11].

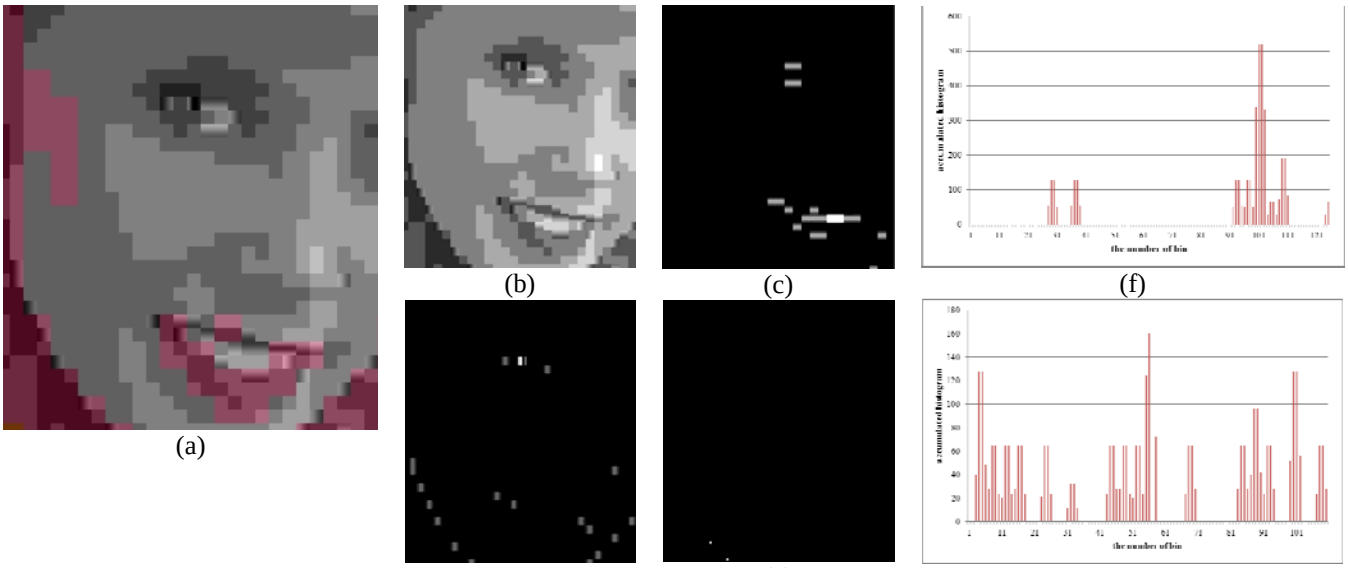

(a) (b) (c) (f) (d) (e) (g)

Fig. 4 (a) highly compressed 'womanhat' image, (b)-(e) wavelet transformed images: (b) approximated image; (c) horizontal detailed image; (d) vertical detailed image; (e) diagonal detailed image, (f) accumulated histogram of horizontal image into vertical direction, (g) accumulated histogram of vertical image into horizontal direction.

The results show that all the metrics including the proposed metric can predict the perceived blockiness of images for same content.

In order to evaluate the performance of the metrics, we followed the recommendations of the VQEG [13]. We used the four performance measures including Pearson correlation coefficient (PCC), Spearman rank-order correlation coefficient (SROCC), mean absolute error (MAE), and root mean squared error (RMSE). Note that, for a well-defined metric, the values of PCC and SROCC should be high and the values of MAE and RMSE should be low.

The results are given in Table 1 for LIVE JPEG image database (Test 2). The results show that the proposed metric provides remarkable performance with higher correlation than 0.9. In addition, the proposed metric outperforms the other existing metrics. LABM [7] is only one competitive metric to the proposed metric that provides relatively high correlation 0.897. However, it requires more complex procedures in LABM, such as local contrast masking and spatial masking.

Table 1 The performance results for LIVE database

	PCC	SROCC	MAE	RMSE
Proposed	**0.911**	**0.871**	**10.915**	**14.560**
GBIM [4]	0.740	0.731	19.255	23.699
BBAM [6]	0.850	0.805	14.581	18.569
LABM [7]	0.897	0.860	11.472	15.089
PBM [11]	0.724	0.825	31.086	35.221

IV. CONCLUSION

In this paper, a new metric is proposed for measuring the blocking artifact based on the properties of the horizontal and vertical detailed images in wavelet domain. The experimental results show that the proposed metric provides remarkable performance for predicting the perceived blockiness of JPEG-compressed images. Future research includes the improvement of the proposed metric, e.g. the responses of human visual system on the blocking artifact should be considered.

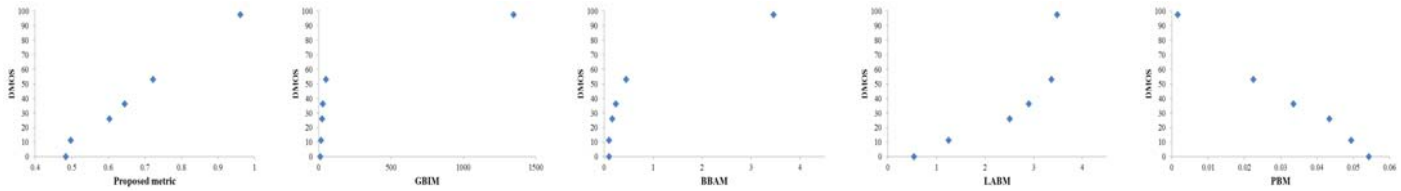

(a) (b) (c) (d) (e)

Fig. 5 results of blockiness metrics when applied to 'womanhat' images with different MOS: 0 (original), 11.31, 25.84, 36.28, 52.92, and 97.51: (a) proposed metric; (b) GBIM [4]; (c) BBAM [6]; (d) LABM [7], (e) PBM [10-11].

REFERENCES

[1] C. Koh, S. Mitra, J. Foley, and I. Heyndericx, "Annoyance of indivisual artifacts in MPEG-2 compressed video and their relation to overall annoyance," *Proc. of the SPIE*, San Jose, CA, Jan. 2005.

[2] H. R. Wu and K. R. Rao, *Digital Video Image Quality and Perceptual Coding*, CRC press, Inc., Boca Raton, FL, 2006.

[3] Z. Wang and A. C. Bovik, *Modern Image Quality Assessment*, Morgan & Claypool, USA, 2006.

[4] H. R. Wu and M. Yuen, "A generalized block-edge impairment metric for video coding," *IEEE Signal Processing Letters*, vol. 4, no. 11, pp. 317-320, Nov. 1997.

[5] J. Yang, H. Choi, and T. Kim, "Noise estimation for blocking artifacts reduction in DCT coded images," *IEEE Transactions on Circuits and Systems for Video Technology*, vol. 10, no. 7, pp. 1116-1120, Oct. 2000.

[6] Z. Wang, A. C. Bovik, and B. Evan, "Blind measurement of blocking artifacts in images," *Proc. IEEE International Conference on Image Processing (ICIP)*, Vancouver, BC, Canada, Sep. 2000.

[7] F. Pan, X. Lin, S. Rahardja, W. Lin, E Ong, S Yao, Z Lu, and X. Yang, "A locally adaptive algorithm for measuring blocking artifacts in images and videos," *Signal Processing: Image Communication*, vol. 19, no. 6, pp. 499-506, Jul. 2004.

[8] I. Kirenko, and R. Muijs, "Coding artifact reduction using non-reference block grid visibility measure," *Proc. IEEE International Conference on Multimedia and Expo (ICME)*, Toronto, Ont. Canada, Jul. 2006.

[9] G. Zhai, W. Zhang, X. Yang, W. Lin, and Y. Xu, "No-reference noticeable blockiness estimation in images," *Signal Processing: Image Communication*, vol. 23, no. 6, pp. 417-432, Jul. 2008.

[10] H. Liu, and I. Heynderickx, "A no-reference perceptual blockiness metric," *Proc. IEEE International Conference on Acoustics, Speech and Signal Processing (ICASSP)*, Las Vegas, NV, Mar. 2008.

[11] H. Liu, and I. Heynderickx, "A perceptually relevant no-reference blockiness metric based on local image characteristics," *EURASIP Journal on Advances in Signal Processing*, vol. 2009, no. 263540, pp. 1-14, Jan. 2009.

[12] H. R. Sheikh, Z. Wang, L. Cormack, and A. C. Bovik, "LIVE image quality assessment database release 2," 2006, http://live.ece.utexas.edu/research/quality.

[13] VQEG, "Final report from the Video Quality Experts Group on the validation of objective models of video quality assessment Phase II," Aug. 2003.